Physics Letters A 378 (2014) 2382–2388

Contents lists available at ScienceDirect

Physics Letters A

www.elsevier.com/locate/pla

Impact of the recorded variable on recurrence quantification analysis of flows

Leonardo L. Portes [a,*], Rodolfo N. Benda [a], Herbert Ugrinowitsch [a], Luis A. Aguirre [b]

[a] Escola de Educação Física, Fisioterapia e Terapia Ocupacional, Universidade Federeal de Minas Gerais, Av. Antônio Carlos 6627, 31270-901 Belo Horizonte MG, Brazil

[b] Departamento de Engenharia Eletrônica, Universidade Federeal de Minas Gerais, Av. Antônio Carlos 6627, 31270-901 Belo Horizonte MG, Brazil

ARTICLE INFO

Article history:
Received 3 January 2013
Received in revised form 7 June 2014
Accepted 9 June 2014
Available online 12 June 2014
Communicated by C.R. Doering

ABSTRACT

Recurrence quantification analysis (RQA) is useful in analyzing dynamical systems from a time series $s(t)$. This paper investigates the robustness of RQA in detecting different dynamical regimes with respect to the recorded variable $s(t)$. RQA was applied to time series $x(t)$, $y(t)$ and $z(t)$ of a drifting Rössler system, which are known to have different observability properties. It was found that some characteristics estimated via RQA are heavily influenced by the choice of $s(t)$ in the case of flows but not in the case of maps.

1. Introduction

Biological systems are complex as they have a huge number of components and degrees of freedom that interact with the environment in subtle ways. Mathematical modeling and analysis of such systems is a challenge. Interactions with the environment or with another system that result in a qualitatively different dynamics, can be represented by a change in a bifurcation parameter. In the case of relatively slow changes, this leads to a drifting behavior which is a common type of nonstationarity, an additional difficulty that has to be dealt with in practice [1–3]. Often, the measurement process itself restricts the type of analyses that can be performed, because it gives access only to a few variables of the system.

The ability of recurrence plots (RPs) and recurrence quantification analysis (RQA) to localize bifurcation behavior in drifting systems, without any a priori hypothesis of the equations of motion, is known [4–7]. By "drifting" we mean slowly time-varying. These features are particularly important in the analysis of data series of biological systems, intrinsically nonstationary. Originally, RPs were introduced to visually distinguish different dynamical behaviors in time series, since periodic, chaotic and random behaviors generate distinct structures in the RPs [4]. Subsequently, RQA was introduced to quantify the properties of RPs [5]. One of the first demonstrations of RQA capabilities was a windowed analysis of the times series of a drifting logistic map, in which several RQA variables were sensitive to bifurcation behavior [6]. The RQA detection of bifurcations, discussed in the context of maps [6], has been applied to time series of flows, not only to detect bifurcations, but also to quantify other dynamical features [3,8,9]. Unfortunately, some characteristics calculated using RQA are very sensitive to user-specified parameters, such as recurrence thresholds, and there is no agreement as how to choose such parameters [7].

Recently, a link was established between observability and embedding theory, demonstrating that the effectiveness of numerical algorithms in quantifying the dynamical features of a system is sometimes highly determined by the variable chosen to reconstruct its dynamics [10–12].

Given the growing importance of RQA in a number of simulated and experimental problems, it is only natural to wonder to what extent does the choice of the recorded variable influence the performance of RQA. In the present work, such robustness is investigated, thus illustrating that observability might influence RQA. In addition to this, another contribution of this work is the investigation of the aforementioned issues in the context of *flows* rather than maps, as discussed in [6]. To this end, the drifting Rössler system is used because of its clear-cut observability properties. The reported results show that, depending on the recorded variable used, some transitions between dynamic regimes are less visible when RQA is performed and some are especially hard to detect.

The present work is organized as follows. Section 2 provides some background. The procedure to generate three time series of the drifting Rössler system, for each of the variables x, y and z is defined in Section 3. Such variables can be ranked as $y \triangleright x \triangleright z$ in terms of observability [11,12]. In Section 4 it is found that some characteristics of RQA are insensitive to bifurcations when the variable z is used. The RQA variables are evaluated using the Poincaré

* Corresponding author. Tel.: +55 31 3409 2394.
E-mail address: ll.portes@gmail.com (L.L. Portes).

http://dx.doi.org/10.1016/j.physleta.2014.06.014
0375-9601/

section of the flow in Section 5, in order to compare the impact of the variables chosen to reconstruct the dynamics on the RQA of flows and maps. The results are discussed in Section 6 and the main conclusions are pointed out in Section 7.

2. Background

2.1. Observability

In this section we briefly review the observability coefficients as defined in [11]. Consider the autonomous system $\dot{\boldsymbol{x}} = f(\boldsymbol{x})$, where $\boldsymbol{x} \in \mathbb{R}^n$ is the state vector and $f : \mathbb{R}^n \mapsto \mathbb{R}^n$ is the vector field. Consider further the measuring function $h : \mathbb{R}^n \mapsto \mathbb{R}$ such that $s(t) = h(\boldsymbol{x})$, where $s \in \mathbb{R}$ is the observable. Differentiating $s(t)$ yields

$$\dot{s}(t) = \frac{d}{dt}h(\boldsymbol{x}) = \frac{\partial h}{\partial \boldsymbol{x}}\dot{\boldsymbol{x}} = \frac{\partial h}{\partial \boldsymbol{x}}\boldsymbol{f}(\boldsymbol{x}) = \mathcal{L}_f h(\boldsymbol{x}), \tag{1}$$

where $\mathcal{L}_f h(\boldsymbol{x})$ is the Lie derivative of h along the vector field $\boldsymbol{f}$. The jth-order Lie derivative is given by [13, p. 8]:

$$\mathcal{L}_f^j h(\boldsymbol{x}) = \frac{\partial \mathcal{L}_f^{j-1} h(\boldsymbol{x})}{\partial \boldsymbol{x}} \cdot \boldsymbol{f}(\boldsymbol{x}), \tag{2}$$

where $\mathcal{L}_f^0 h(\boldsymbol{x}) = h(\boldsymbol{x})$. The time derivatives of s can be written in terms of Lie derivatives as $s^{(j)} = \mathcal{L}_f^j h(\boldsymbol{x})$. The observability matrix can be written as [14]:

$$\mathcal{O}_s(\boldsymbol{x}) = \begin{bmatrix} \frac{\partial \mathcal{L}_f^0 h(\boldsymbol{x})}{\partial \boldsymbol{x}} \\ \vdots \\ \frac{\partial \mathcal{L}_f^{m-1} h(\boldsymbol{x})}{\partial \boldsymbol{x}} \end{bmatrix}, \tag{3}$$

where the index s indicates that $\mathcal{O}_s(\boldsymbol{x})$ refers to the system observed from $s(t)$. The system is observable from $s(t)$ if $\mathcal{O}_s(\boldsymbol{x})$ is full rank. This classical definition of observability yields "yes–no" answers and poorly observable systems are (correctly) classified as observable.

In order to rank the quality of the system variables in conveying dynamical information, it is helpful to assess how far is $\mathcal{O}_s(\boldsymbol{x})$ from being rank-deficient. This can be achieved computing a coefficient δ_s that quantifies the numerical ill-conditioning of such a matrix along a trajectory $\boldsymbol{x}(t)$ when the recorded variable is $s(t)$. Hence

$$\delta_s(\boldsymbol{x}) = \frac{|\lambda_{\min}[\mathcal{O}_s(\boldsymbol{x})^T \mathcal{O}_s(\boldsymbol{x})]|}{|\lambda_{\max}[\mathcal{O}_s(\boldsymbol{x})^T \mathcal{O}_s(\boldsymbol{x})]|}, \tag{4}$$

where $\lambda_{\max}[\mathcal{O}_s(\boldsymbol{x})^T \mathcal{O}_s(\boldsymbol{x})]$ indicates the maximum eigenvalue of matrix $\mathcal{O}_s(\boldsymbol{x})^T \mathcal{O}_s(\boldsymbol{x})$ estimated at point $\boldsymbol{x}(t)$ (likewise for $\lambda_{\min}$). Then $0 \leq \delta(\boldsymbol{x}) \leq 1$, and the lower bound is reached when the system is not observable at point $\boldsymbol{x}$. Coefficient $\delta_s(\boldsymbol{x})$ in (4) is a type of condition number of the matrix $\mathcal{O}_s(\boldsymbol{x})^T \mathcal{O}_s(\boldsymbol{x})$. Averaging $\delta_s(\boldsymbol{x})$ along a trajectory over the interval $t \in [0;\ T]$ yields the observability coefficient

$$\delta_s = \frac{1}{T}\sum_{t=0}^{T} \delta_s\big(\boldsymbol{x}(t)\big). \tag{5}$$

The challenges of evaluating observability from data, i.e. without knowing the system equations, have been discussed in [12].

2.2. Recurrence quantification analysis

The RQA technique was initially proposed by Webber and Zbilut [5,15] to quantify the qualitative information of recurrence plots (RP) formulated by Eckmann et al. [4]. Given a time series $\{x\}$, a recurrence matrix $\mathbf{R}_{i,j}(\epsilon)$ is constructed by the N time-ordered embedded vectors in m-dimensional space $\{\vec{X}_i\}_1^N \in \mathbb{R}^m$ by the rule [7]:

$$\mathbf{R}_{i,j}(\epsilon) = \Theta\big(\|\vec{X}_i - \vec{X}_j\| - \epsilon\big), \quad i, j = 1, ..., N. \tag{6}$$

A recurrence situation happens when the distance between $\vec{X}_i$ and $\vec{X}_j$ is less than a threshold ϵ. In that case, the Heaviside Θ function returns 1, otherwise it returns 0. The typical RP is a diagram of $\mathbf{R}_{i,j}(\epsilon)$ where black dots are used to indicate the 1s and the 0s are left blank.

The recurrence structure of $\mathbf{R}_{i,j}(\epsilon)$ can be quantified by indices, some of which are presented in the sequel. The density of recurrent points in the RP is the recurrence rate, often expressed in percentage as:

$$\%REC = \frac{1}{N^2}\sum_{i,j=1}^{N} \mathbf{R}_{i,j}(\epsilon) \times 100\%. \tag{7}$$

The so called "determinism" coefficient is the percentage of recurrent points that form diagonal lines with minimum length $l_{\min}$

$$\%DET = \frac{\sum_{l=l_{\min}}^{N} lP(l)}{\sum_{l=1}^{N} lP(l)} \times 100\%, \tag{8}$$

where $P(l)$ is the frequency distribution of diagonal lines of length l parallel to the identity line. $l_{\min}$ must be small because a large value could result in a sparse histogram $P(l)$. On the other hand, $l_{\min}$ should be sufficiently large to exclude the diagonal lines formed by tangential motion of the trajectory in phase space [7].

The Shannon entropy of line segment distributions was defined as

$$ENTR = -\sum_{l=l_{\min}}^{N} p(l)\ln p(l), \tag{9}$$

and is based on the probability that a diagonal line in the RP has length l, that is, $p(l) = P(l)/N_l$, where N_l is the total number of valid lines ($l \geq l_{\min}$).

The inverse of the longest diagonal line is by definition the divergence

$$DIV = \big(\max\big(\{l_i\}_{i=1}^{N_l}\big)\big)^{-1}, \tag{10}$$

which is expected to be correlated to the largest Lyapunov exponent $\lambda_{\max}$ [4,6,16].

An index related to (9) was defined as [17]

$$S = -\sum_{l=1}^{N} P_{\mathrm{nr}}(l)\ln P_{\mathrm{nr}}(l), \tag{11}$$

where $P_{\mathrm{nr}}(l)$ is the number of diagonal lines formed by *nonrecurrent* points ($R_{i,j} = 0$) divided by the number of *recurrent* points. A correction to the algorithm in [17] is given by the same author at http://www.atomosyd.net/spip.php?article74.

2.3. Numerical setup

In order to investigate the impact of the recorded variable on RQA, a benchmark system plus a set of indices must be chosen.

Trulla et al. [6] applied the RQA to a drifting logistic equation and reported that the indices (7)–(10) are sensitive to the dynamical regime, and therefore can be used to indicate the transitions: periodic–periodic, periodic–chaotic and chaotic–periodic. Hence a drifting system seems adequate as a benchmark for RQA. Because one of the objectives of this work is to investigate the effects

observability on RQA in the context of flows and maps, the benchmark chosen was the Rössler system with a slowly varying parameter (described in Section 3) for which the observability properties are well known.

As for the indices to be used in RQA, it is natural to start with (7)–(10) because such were originally used for this purpose [7] – in addition to a fifth one, TREND. This index, also used in [6], measures the fading of recurrence points away from the central diagonal line and is highly sensitive to user-defined parameters and, therefore, was not used in the present investigation.

Another interesting aspect of [6] is that it reports two unexpected results related to Eq. (9), namely: (i) *ENTR* was *lower* in chaotic than in periodic regimes, and (ii) *ENTR* was *proportional to the inverse* of $\lambda_{\max}$. However, Shannon's entropy is expected to increase with the system's complexity and to be proportional to $\lambda_{\max}$ [18]. The findings reported in [6] are rather counterintuitive because *ENTR* is usually interpreted as an entropy and this interpretation leads to paradoxal results [6,9,19].

In view of such results, in addition to *ENTR* the index S in (11), which is clearly related to Shannon's entropy, will also be used in this work. Hence, (7)–(10) and (11) will be computed from the three time series obtained by simulating the benchmark system described in what follows.

3. Drifting Rössler system

In order to mimic the complex behavior of biological systems, with transients and drifts, and to study the impact of observability on RQA, following [6], we will perform the analysis on a time-varying benchmark in nonlinear dynamics, the Rössler system [20]:

$$\begin{aligned}\dot{x} &= -y - z,\\ \dot{y} &= x + ay,\\ \dot{z} &= b + z(x - c)\end{aligned} \tag{12}$$

where (a, b, c) are parameters. Unlike Trulla et al. [6], who reported results for a *map*, in this section the case of a *vector field* will be investigated.

The following steps were performed to produce drifting time series of the x, y and z variables:

1. set the parameters $(a, b, c) = (0.3, 2, 4)$ and the final value of parameter a, a_f. Set the initial condition, e.g. $(x_o, y_o, z_o) = (2, 0, 0)$ and the integration time $t = 0$;
2. update the time $t \leftarrow t + \delta t$;
3. integrate (12) with initial condition (x_o, y_o, z_o) up to time t and record the point (x_t, y_t, z_t);
4. increase the bifurcation parameter a by 0.0000003, that is, set $a_{\text{new}} \leftarrow a_{\text{prev}} + 3 \times 10^{-7}$, and take as the new initial condition $(x_o, y_o, z_o) \leftarrow (x_t, y_t, z_t)$;
5. return to step 2 while $a_{\text{new}} \leq a_f$.

Integration was performed with Mathematica function NDSolve which works with an adaptive integration interval (Wolfram Research Inc., Champaign IL, USA). The algorithm was iterated for $a \in [0.3, 0.55]$ $(a_f = 0.55)$ for a total evolution time of $\Delta T = 166{,}667$. The range $a \in [0.3, 0.55]$ was chosen in order to visit different dynamical regimes such as periodic–periodic, periodic–chaotic, chaotic–periodic and chaotic–chaotic. The sampling interval $T_s = 0.6$. This produced time series of x and y and z with length $N = 277{,}778$ points each.

The bifurcation diagram of the drifting Rössler system is plotted as functions of the bifurcation parameter a in Fig. 1. The values used in the bifurcation diagram were obtained by estimating the intersections of the trajectory with the Poincaré section:

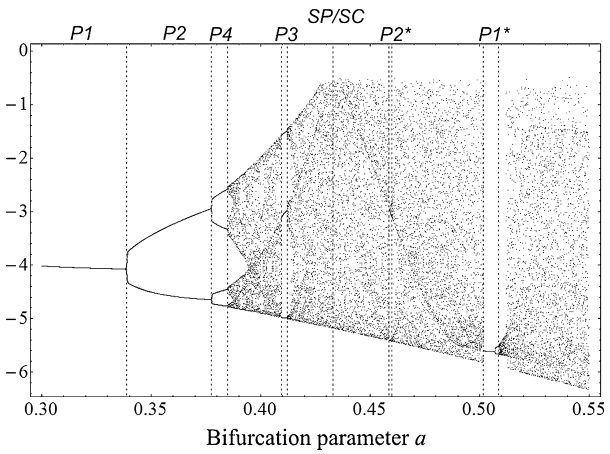

Fig. 1. Bifurcation diagram of the drifting Rössler system computed over $\Delta T = 166{,}667$. The vertical lines highlight some of the changes in the dynamical regime: periodic–periodic, periodic–chaotic, chaotic–periodic and spiral-type/screw-type chaos, for fixed parameters $(b, c) = (2, 4)$.

$$\mathcal{P} \equiv \left\{(y, z) \in \mathbb{R}^2 \;\middle|\; x = x_c, \dot{x} > 0\right\}, \tag{13}$$

where x_c is the coordinate of the fixed point located in the middle of the attractor. Although the integration step used is small, the probability that a discrete-time value of the trajectory falls exactly on $\mathcal{P}$ is zero. Calling $\vec{X}_{i-2}, \vec{X}_{i-1}, \vec{X}_i, \vec{X}_{i+1}$ the sequence of vectors in phase space such that $\vec{X}_{i-2}, \vec{X}_{i-1}$ are the two last vectors just *before* the trajectory crosses $\mathcal{P}$ and $\vec{X}_i, \vec{X}_{i+1}$ are the two first vectors just *after* having crossed the Poincaré section. A polynomial was fitted to the working data ($T_s = 0.6$) using Mathematica `InterpolatingPolynomial` function: $\vec{X}_{i-2}, \vec{X}_{i-1}, \vec{X}_i, \vec{X}_{i+1}$ and used to estimate $\vec{X}_{\mathcal{P}}$, the location where the continuous trajectory would have crossed $\mathcal{P}$. This was performed every time the trajectory crossed $\mathcal{P}$. It is pointed out that linear interpolation is usually sufficient for this purpose, especially when the sampling time is very small.

In what follows, the aim will be to detect, using RQA, the more visible changes in dynamical regimes highlighted by the vertical lines (Fig. 1): period-1 (P1), period-2 (P2) and period-4 (P4) regimes, periodical windows period-3 (P3) and period-1 (P1*) embedded in chaos, and finally the spiral-chaos/screw-chaos (SP/SC). The values of the bifurcation parameter a corresponding to the vertical lines are 0.3388, 0.3774, 0.3848, 0.4095, 0.4121, 0.43295, 0.4585, 0.4598, 0.5017 and 0.5086. The SP/SC is not a bifurcation, but a transition to multimodal chaos [21].

4. RQA of the drifting Rössler system

RQA of the drifting Rössler system was performed embedding each of the time series $\{x\}$, $\{y\}$ and $\{z\}$ in a 3D time-delay embedding space [7]. If the data were stationary, RQA would be implemented using the entire time series. Because the data are nonstationary, due to the drift in parameter a, RQA is performed on a running window of length W.

A sensitivity study was performed in order to assess the influence of ϵ (see Eq. (6)) and of W on the RQA results. It was found that the results were quite similar when such parameters were taken within the ranges: $0.4 \leq \epsilon \leq 1.4$ and $400 \leq W \leq 1200$. In what follows, the chosen window length was $W = 800$ with increments of 10 data points between successive windows. There is no clear agreement in the literature about how to choose ϵ as pointed out in [7]. A rule of thumb is that such a value should not exceed 10% of the mean or maximum phase space diameter [7,15]. In this work, the threshold ϵ was chosen as $\epsilon_x = \epsilon_y = 0.6$ and $\epsilon_z = 0.9$, which correspond to approximately 5% of the greatest

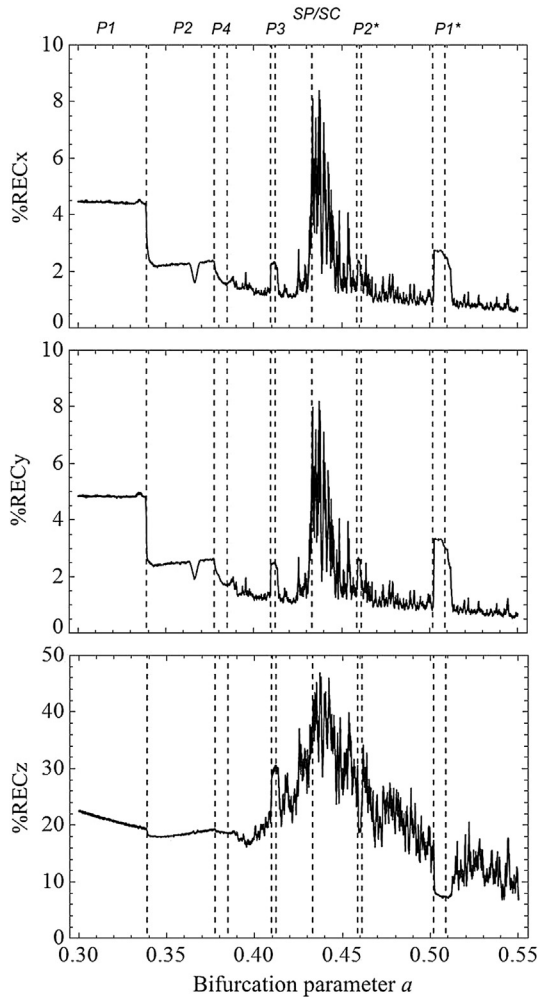

Fig. 2. *%REC* variable computed from data of the drifting Rössler system: x (top), y (middle) and z (bottom). In several cases the changes to different dynamical regimes are less visible in the bottom plot due to poor observability. The vertical lines indicate the bifurcation points (see Fig. 1).

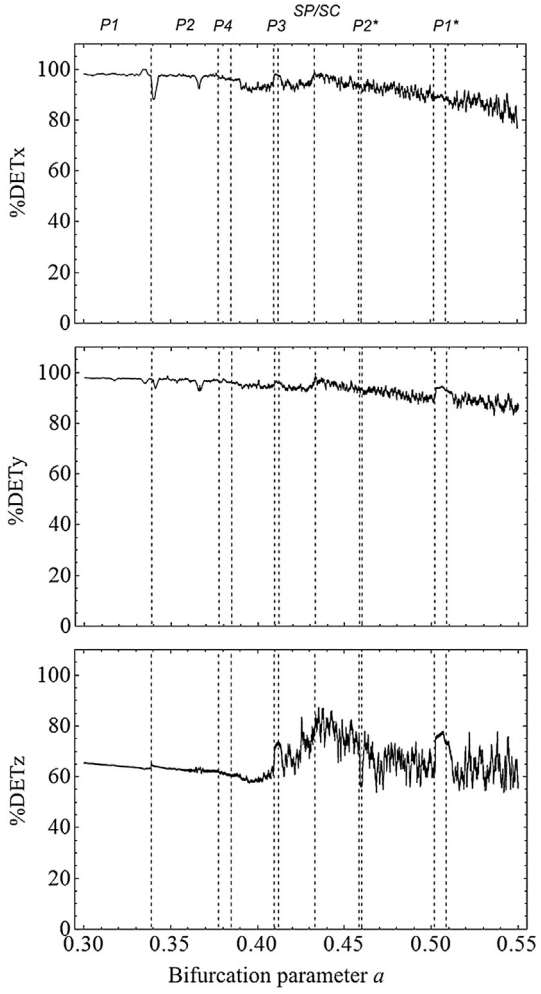

Fig. 3. *%DET* computed from the three time series.

distance in the respective reconstructed phase space $D_{\max}$. $l_{\min} = 2$ was used for the computation of %DET, corresponding to 1/5 of the pseudo-period of the flow, which eliminates the influence of laminar motion due to oversampling.

Finally, for each epoch (27,697 windows altogether) the characteristics (7)–(11) were estimated. These were chosen because they are known to be sensitive to changes in the dynamical regime [6,7].

Some features are expected when plotting the RQA variables against the bifurcation parameter [6,17]: (i) clear alterations at bifurcating points; (ii) *%REC* and *%DET* being higher in the periodic dynamic regimes than in the chaotic ones; (iii) *S* and *DIV* being lower in the periodic windows; (iv) ENTR being higher in the periodic windows [6,7] because it is believed to be correlated with the inverse of the complexity of the dynamics. Note that the different RQA variables characterize different dynamical aspects [7,22]. Therefore, it is to be expected that these variables behave differently and that some of them identify certain transitions whereas other variables identify other transitions. For the RQA variables used in the present investigation, its not expected that DIV should detect period–period transitions, as DIV is claimed to be strongly linked to the Lyapunov exponent.

Fig. 2 shows *%REC* computed for the time series x, y and z. The same vertical lines of Fig. 1 are shown to help check the coincidence of the RQA-estimated bifurcations and those of Fig. 2. Note that the scales differ. As seen, *%REC* has visible alterations at the transitions P1/P2, P3 and P1* for all time series. Although the periodic dynamical regime P1* is clear in the plots obtained from all time series, in the one from the z variable, it is noted that *%REC* is *lower* in the periodic regime. This unexpected behavior may be attributed to the very poor observability provided by the z variable. Strictly speaking the same happens for P2*, although the changes in *%REC* are hard to distinguish from the noise-like background for all the time series. As for P2/P4, the changes in $\%REC_{x,y}$ are clearly more visible than that in $\%REC_z$, where there is practically no change. The large peak at the SC/SP is due to the fact that the trajectory falls very close to the fixed point and remains in its neighborhood for a long time [21]. Such a peak is very visible with x and y, but less visible with z because it blends with the background which is due to the low observability of z. If the transition SP/SC had not been known *a priori*, it is arguable if the large fluctuations in $\%REC_{x,y}$ around such a bifurcation would be credited to it. Finally, the several small peaks could result from unstable periodic orbits or tiny periodic windows, which are not visible in the bifurcation diagram.

The *%DET* index, Eq. (8), is shown in Fig. 3. If such an index quantified *determinism* proper, the expected behavior would be a straight line at 100%. Therefore, other issues, such as numerical ones and predictability, should account for variations in *%DET*. The deviation from 100% is clearly seen when *%DET* is computed using the z time series and even increases in the chaotic region. The behavior when y is used is (slightly) better than with x and both are much closer to 100% than for the results obtained using z. These

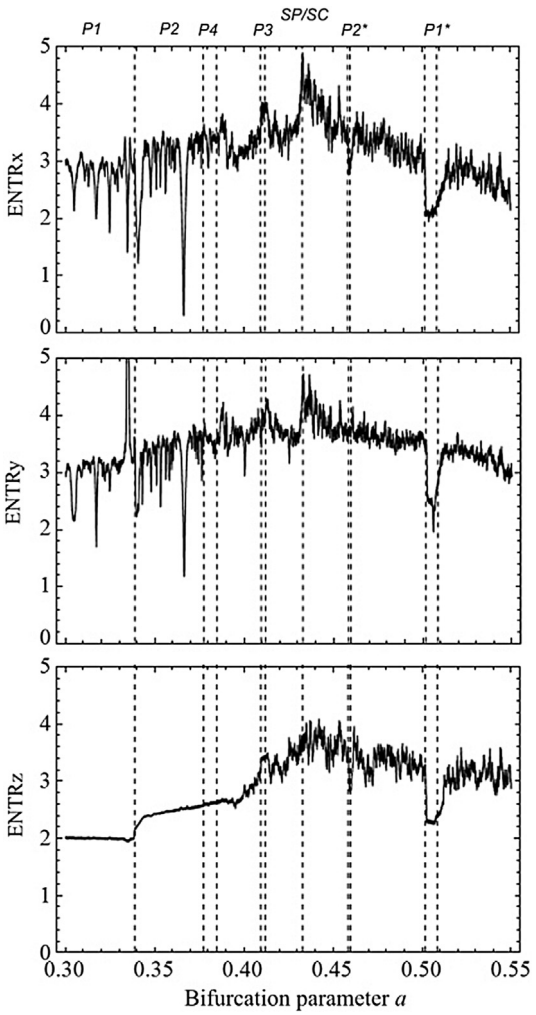

Fig. 4. The "Shannon" entropy of diagonal line distribution *ENTR* shows inconsistent behavior.

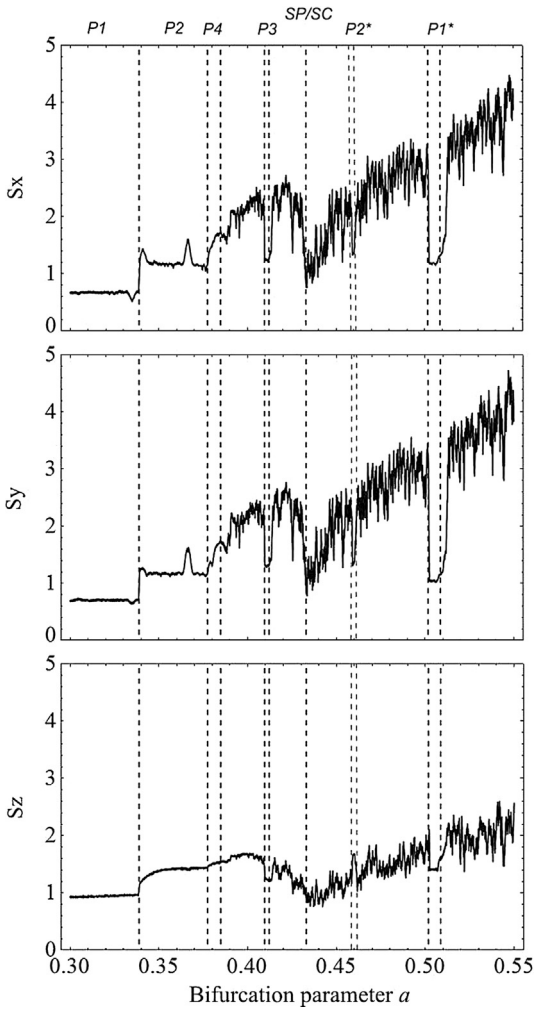

Fig. 5. The Shannon entropy S. The bottom plot is far smoother than the other two. This is probably due to the poor observability provided by the z time series.

features are again in agreement with the ranking of the variables of the Rössler system in terms of observability $y \triangleright x \triangleright z$ [11,12]. The higher value of $\%DET_z$ in P1* than in P1 is due to the fact that the trajectory in P1* has greater projection on the z-axis than in P1 [21].

The index *ENTR* (Fig. 4) is rather inconsistent as a discriminator of RP complexity [6,7]. For example, *ENTR* for the periodic regime P3 is higher than for P1, P2 and P1*, which seems to be in agreement with the fact that the latter are dynamical regimes with simpler dynamics than P3. On the other hand, *ENTR* for P4 window and for the chaotic regimes between P4 and P3 is *lower* than for P3 (which has a simpler dynamics). Other instances of such inconsistency can be found in Fig. 4 regardless of the time series chosen to reconstruct the dynamics (with minor differences in z).

The entropy S, shown in Fig. 5 is "smoother" when computed from the z variable. As a consequence of this smoothing effect–similar to that of *%REC* (Fig. 2), dynamical changes in the system are not so clearly revealed when the analysis is carried out using z. This is consistent with the low observability provided by z. Note that S_x and S_y are almost identical. The periodic windows P1, P2, P3 and P1* are highly visible with x and y, which is clearly not the case with z. The same can be seen with the abrupt fall of the entropy due to the SP/SC transition, which is less visible in S_z. P2* is marked by a small valley in $S_{x,y}$, but is not visible in S_z.

The variable *DIV*, Fig. 6, had the behavior similar of the RQA of the logistic map [6]: all periodic windows had very low values of *DIV*, close to 0.001 and chaotic windows had higher values. This coefficient is clearly very robust to the choice of the recorded variable, which would strongly recommend its use. On the other hand, *DIV* is unable to detect periodic–periodic and chaos–chaos changes in the dynamical regime.

5. RQA on a Poincaré section

Observability, as defined in Section 2.1, has no practical effect on the analysis when measurements are taken on a Poincaré section [17]. In order to evaluate such a remark in the context of RQA, the analysis was performed using data on the Poincaré section defined in Eq. (13) applied to the drifting Rössler system. Scalar time series $\{y_n\}$ and $\{z_n\}$ were obtained from the Poincaré section (13) and processed using a running window of length $W = 200$ with increments of 10 data points between successive windows. The sets were time-delay embedded in 3D space with time lag $\tau = 2$ (both parameters were confirmed by false neighbors and mutual information techniques, respectively). The RQA parameters were $\epsilon_y = 0.1$ and $\epsilon_z = 0.15$ (approximately 5% of the greatest distance in the respective reconstructed phase space) and $l_{\min} = 2$.

Fig. 7 shows *%REC* and *%DET*, and Fig. 8 shows *ENTR* and *DIV*. The quality of S was roughly the same regardless of the variable chosen to reconstruct the dynamics, as found in [17]. Note that the behavior of *ENTR* is now consistent over the different dynamical regimes, in the sense that it is correlated to the inverse of the complexity of the dynamics, but the peak at P3 is less visible

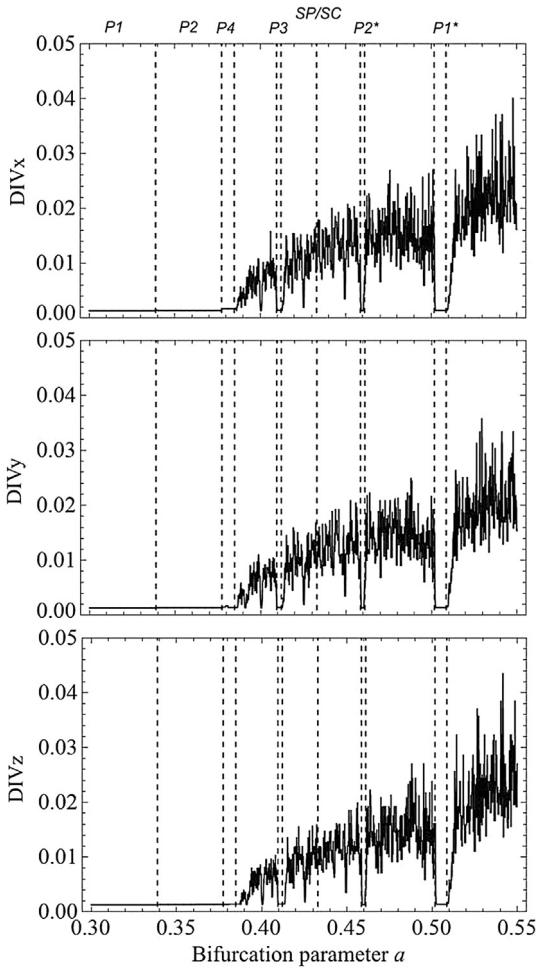

Fig. 6. The divergence is noisy, but is not affected by the choice of recorded variable.

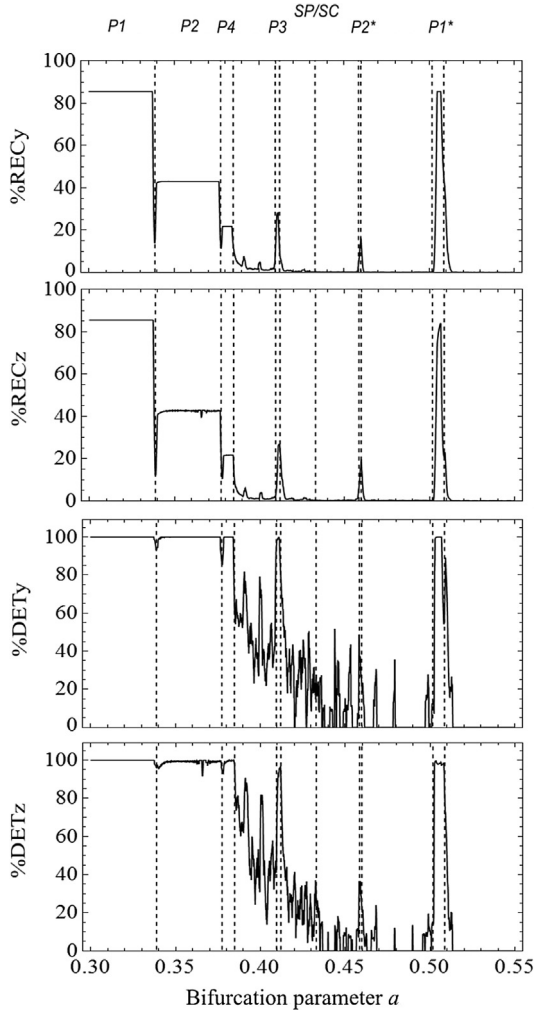

Fig. 7. *%REC* and *%DET* variables computed from the Poincaré section data $\{y_n\}$ and $\{z_n\}$.

when computed with z than with y. The same degradation at the transition P2/P4 using z. Theoretically (Section 2.1), y and z taken on a Poincaré section should give indices of comparable quality, as shown here with *%REC*, *%DET* and *DIV* and S in [17]. Hence, once again *ENTR* does not seem helpful for the purposes of the present investigation.

In closing this section we point out that a counterpart interpretation of observability in the case of Poincaré section data is related to the definition of the section itself and *not* to the choice of the observable used in the analysis, as the results (in this paper and in [17]) clearly show. Hence, varying observability features for maps would be obtained if the Poincaré section were gradually turned from a position orthogonal to the flow to one that is tangent to it (when it would no longer be a Poincaré section).

6. Discussion

The drifting Rössler system was used to investigate if observability properties affect RQA in detecting bifurcations from a drifting time series. The RQA coefficients used were affected in different degrees by observability issues. Changes in dynamical regimes are not so clearly revealed by *%REC* and S when computed from z, which yields poor observability of the system. This corroborates a similar result found in [17] when computing S. On the other hand, *DIV* is very robust with respect to observability properties despite the fact the it is ineffective in detecting periodic–periodic bifurcations.

An unexpected effect found was the valley in *%REC* of the P1* window computed with z (Fig. 2), in contrast with the peaks when computed with x and y, that could lead to wrong conclusions about the system's dynamics. The same was found for P2*, but less visible. This effect can be understood observing the different points of view of the dynamics expressed in Fig. 9. More information about the dynamics can be seen at the perspective (b) than at (c), in which the region of low observability (LOB) gives the wrong information of high recurrence to the RQA algorithm. So, poor observability can result in a less contrasting behavior on RQA variables during changes in the dynamical regime.

It should be pointed out that interpreting the index in Eq. (8) as a measure of determinism raises some difficulties. In the analyses of the logistic map in [6], *%DET* was 100% only in the periodic windows, falling to values near 40% in chaos which is misleading, because the dynamics of the logistic map is always deterministic. However, as mentioned just before Eq. (8) such an index actually quantifies *recurrent data segments*. In periodic regimes with low periods recurrence is higher than in periodic regimes of higher period, and both are higher than chaos, where the trajectory covers a denser region in phase space therefore reducing recurrence somewhat. This is clearly seen in Fig. 3. In short *%REC* quantifies recurrent points whereas *%DET* recurrent segments. *%DET* has a rather close relation to predictability.

Some unexpected features of *ENTR* suggest that such an index is inadequate to perform the investigation pursued in this paper. The reason for this is perhaps related to the rather uncertain interpretation of *ENTR* as an indicator of complexity. Further investigation

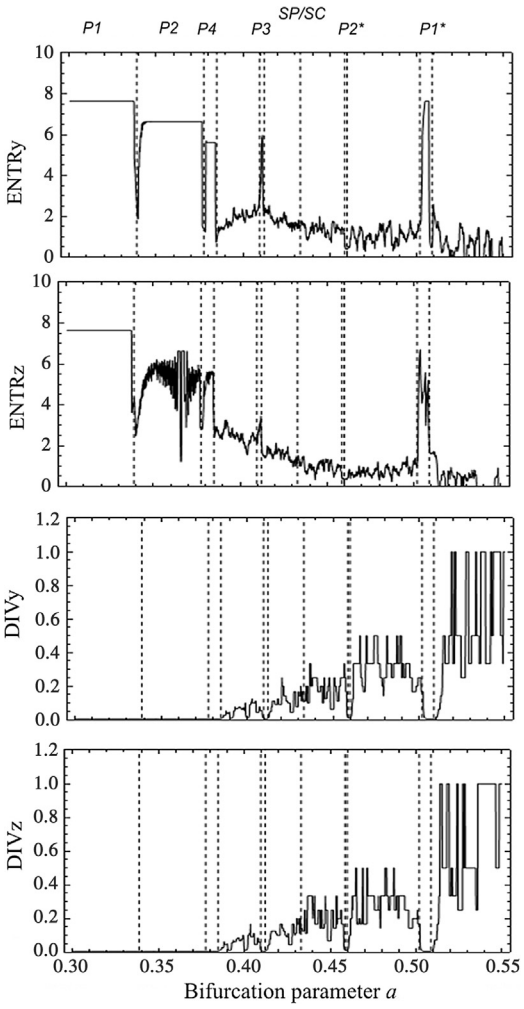

Fig. 8. *ENTR* and *%DIV* variables computed from the Poincaré section data $\{y_n\}$ and $\{z_n\}$.

using a much wider set of systems is required to untangle difficulties of interpretation and possible misconception related to such an index [6,7,17].

When data from a Poincaré section of the flow were used the following was observed: (i) RQA indices were not affected by the observability rank between y and z and (ii) the change of the dynamical regime was more evident.

The entropy S was estimated more accurately from a Poincaré section of a flow (a map), than from the flow data [17]. This has also been verified with other RQA variables, as presented here. This suggests that, whenever possible, the RQA should be performed with data from a Poincaré section of the flow.

7. Conclusion

In real world experiments, especially in biological systems, many recorded variables are at disposal. Criteria used to choose the variable to measure do not usually consider the type of analysis that will be performed. This work has shown that the performance of RQA depends on the characteristics chosen *and* on the recorded variable used. If only one variable has been recorded, the results

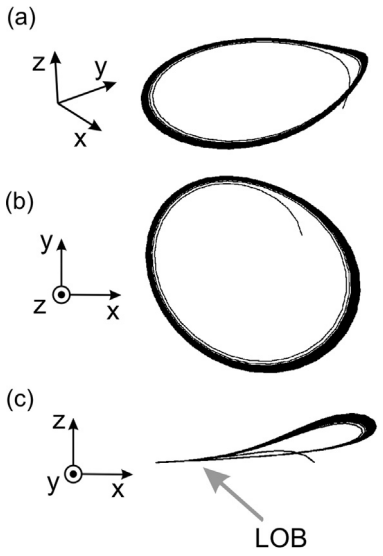

Fig. 9. Different perspectives of the drifting Rössler system, with bifurcation parameter $a = [0.30, 0.32]$.

discussed in this paper show that observability properties of the system through such a variable could be responsible for poor performance of RQA. The main recommendation therefore is to perform data-based observability analysis [12] to choose the recorded variable prior to RQA, whenever possible. A second recommendation is that when dealing with multivariate flows, the performance of RQA can usually be improved by taking data from a Poincaré section, as suggested in [17]. That could be an essential part of the RQA toolkit.

Acknowledgements

The authors gratefully acknowledge financial support from CAPES and CNPq (302079/2011-4).

References

[1] Z. Chen, K. Hu, P. Carpena, P. Bernaola-Galvan, H. Stanley, P. Ivanov, Phys. Rev. E 71 (1) (2005) 011104.
[2] S. Mitra, M.A. Riley, M.T. Turvey, J. Mot. Behav. 29 (3) (1997) 195–198.
[3] M.A. Riley, R. Balasubramaniam, M.T. Turvey, Gait Posture 9 (1999) 65.
[4] J.P. Eckmann, S.O. Kamphorst, D. Ruelle, Europhys. Lett. 5 (1987) 973.
[5] C.L. Webber Jr., J.P. Zbilut, J. Appl. Physiol. 76 (2) (1994) 965.
[6] L.L. Trulla, A. Giuliani, J.P. Zbilut, C.L. Weber Jr., Phys. Lett. A 223 (1996) 255.
[7] N. Marwan, M.C. Romano, M. Thiel, J. Kurths, Phys. Rep. 438 (2007) 237.
[8] M. Aboofazeli, Z.K. Moussavi, Chaos Solitons Fractals 37 (2008) 454.
[9] M.L. Wijnants, A.M.T. Bosman, F. Hasselman, R.F.A. Cox, G.C. Van Orden, Nonlinear Dyn. Psychol. Life Sci. 13 (1) (2009) 75.
[10] C. Letellier, L.A. Aguirre, Chaos 12 (2002) 549.
[11] C. Letellier, L.A. Aguirre, J. Maquet, Phys. Rev. E 71 (2005) 066213.
[12] L.A. Aguirre, C. Letellier, Phys. Rev. E 83 (2011) 066209.
[13] A. Isidori, Nonlinear Control Systems, Springer, London, 1995.
[14] R. Hermann, A.J. Krener, IEEE Trans. Autom. Control 22 (5) (1977) 728.
[15] J.P. Zbilut, C.L. Webber Jr., Phys. Lett. A 171 (3–4) (1992) 199.
[16] M. Thiel, M.C. Romano, P.L. Read, J. Kurths, Chaos 14 (2) (2004) 234.
[17] C. Letellier, Phys. Rev. Lett. 96 (2006) 254102.
[18] Y.B. Pesin, Dimension Theory in Dynamical Systems, University of Chicago Press, Chicago, 1990.
[19] D.G. Stephen, R.A. Boncoddo, J.S. Magnuson, J.A. Dixon, Mem. Cogn. 37 (8) (2009) 1132.
[20] O.E. Rössler, Phys. Lett. A 57 (1976) 397.
[21] C. Letellier, P. Dutertre, B. Maheu, Chaos 5 (1) (1995) 271.
[22] N. Marwan, Int. J. Bifurc. Chaos 21 (2011) 1003.